Oral prion neuroinvasion occurs independently of PrPC expression in the gut epithelium

JVI01010-18-R1

Oral prion neuroinvasion occurs independently of PrP^C expression in the gut epithelium

Running title: Prion disease in mice lacking PrP^C in enterocytes

Alison Marshall[a], Barry M. Bradford[a], Alan R. Clarke[b,c], Jean C. Manson[d#] & Neil A. Mabbott[a#]

[a] The Roslin Institute & Royal (Dick) School of Veterinary Sciences, University of Edinburgh, Easter Bush EH25 9RG, United Kingdom

[b], School of Biosciences, Cardiff University, Museum Avenue, Cardiff CF10 3AX, United Kingdom

[c], Deceased

[d], Centre for Clinical Brain Sciences, University of Edinburgh, United Kingdom

[#] **Address correspondence to:** Jean C. Manson, jean.manson@roslin.ed.ac.uk; Neil A. Mabbott, neil.mabbott@roslin.ed.ac.uk

ABSTRACT The early replication of certain prion strains within the Peyer's patches in the small intestine is essential for the efficient spread of disease to the brain after oral exposure. Our data show that orally-acquired prions utilise specialised gut epithelial cells known as M cells to enter Peyer's patches. M cells express the cellular isoform of the prion protein, PrP^C, and this may be exploited by some pathogens as an uptake receptor to enter Peyer's patches. This suggested that PrP^C might also mediate the uptake and transfer of prions across the gut epithelium into Peyer's patches in order to establish infection. Furthermore, the expression level of PrP^C in the gut epithelium could influence the uptake of prions from the lumen of the small intestine. To test this hypothesis, transgenic mice were created in which deficiency in PrP^C was specifically restricted to epithelial cells throughout the lining of the small intestine. Our data clearly show that efficient prion neuroinvasion after oral exposure occurred independently of PrP^C expression in small intestinal epithelial cells. The specific absence of PrP^C in the gut epithelium did not influence the early replication of prions in the Peyer's patches or disease susceptibility. Acute mucosal inflammation can enhance PrP^C expression in the intestine, implying the potential to enhance oral prion disease pathogenesis and susceptibility. However, our data suggest that the magnitude of PrP^C expression in the epithelium lining the small intestine is unlikely to be an important factor which influences the risk of oral prion disease susceptibility.

IMPORTANCE The accumulation of orally-acquired prions within Peyer's patches in the small intestine is essential for the efficient spread of disease to the brain. Little is known of how the prions initially establish infection within the Peyer's patches. Some gastrointestinal pathogens utilize molecules such as the cellular prion protein, PrP^C, expressed on gut epithelial cells to enter Peyer's patches.

Acute mucosal inflammation can enhance PrP^C expression in the intestine, implying the potential to enhance oral prion disease susceptibility. We used transgenic mice to determine whether the uptake of prions into Peyer's patches was dependent upon PrP^C expression in the gut epithelium. We show that orally-acquired prions can establish infection in Peyer's patches independently of PrP^C expression in gut epithelial cells. Our data suggest that the magnitude of PrP^C expression in the epithelium lining the small intestine is unlikely to be an important factor which influences oral prion disease susceptibility.

Key words prions, transmissible spongiform encephalopathies, PrP, intestine, gut epithelium, Peyer's patches

Introduction

Prions cause chronic neurodegenerative diseases that affect humans and some domesticated and free-ranging animal species to which there are no treatments. Bovine spongiform encephalopathy (BSE) prions also have zoonotic potential (1), exerting high societal and economic costs. The precise nature of the infectious prion is uncertain, but an abnormal, relatively proteinase-resistant isoform (PrP^{Sc}) of the host cellular prion protein (PrP^{C}), co-purifies with prion infectivity in diseased tissues (2), and host cells must express cellular PrP^{C} to sustain prion infection (3).

Many natural prion diseases are acquired by oral consumption of contaminated food or pasture. The gut-associated lymphoid tissues (GALT) within the lining of the intestine such as the tonsils, Peyer's patches, appendix, colonic and caecal patches, together with the mesenteric lymph nodes (MLN), help to provide protection against intestinal pathogens. However, orally-acquired prions exploit the GALT to achieve host infection (4-8). The early replication of prions within Peyer's patches in the small intestine is essential for their efficient spread of from the gut to the brain (termed *neuroinvasion*), as oral prion disease susceptibility is blocked in their absence (5, 9-11).

Orally-acquired prions utilize an elegant cellular relay in the GALT in order to establish host infection. After ingestion, the prions are first transported across the follicle-associated epithelium (FAE) which covers the lumenal surface of the Peyer's patches by M cells (12-16). The prions are then acquired by mononuclear phagocytes within the GALT which they appear to use as "Trojan horses" to shuttle them towards the follicular dendritic cells (FDC) in the B cell follicles (17-19). The subsequent replication of the prions upon FDC is essential for efficient neuroinvasion from the intestine (4, 5, 17, 20). The prions then infect nearby enteric nerves before spreading along fibres of the sympathetic and parasympathetic

nervous systems to the brain where they ultimately cause neurodegeneration and death (17, 21).

M cells are specialized, highly phagocytic, intestinal epithelial cells that facilitate the uptake and trans-epithelial transfer of particulate antigens and microorganisms into the GALT from the gut lumen (22). The transcytosis of particulate antigens by M cells is an important initial step in the induction of efficient mucosal immune responses against certain pathogenic bacteria (23, 24) and the commensal bacterial flora (25). However, some orally-acquired bacterial (26-28) and viral (29, 30) pathogens utilise M cells to achieve host infection. Prions also exploit M cells in order to enter Peyer's patches and establish host infection (13, 16). Furthermore, the density of M cells in the gut epithelium directly limits or enhances disease susceptibility. In the specific absence of M cells, the accumulation of prions in Peyer's patches and subsequent spread of the disease to the brain is blocked (13, 16). In contrast, increased M-cell density at the time of oral exposure enhances prion disease susceptibility approx 10 fold by increasing the uptake of prions from the gut lumen (16).

M cells are considered to express a variety of "immunosurveillance" receptors on their apical surfaces which enable them to acquire certain pathogens and antigens. For example, glycoprotein 2 (GP2) can act as a receptor for $FimH^+$ bacteria such as *Eschericia coli* and *Salmonella enterica* serovar Typhimurium (23). Uromodulin (also known as Tamm-Horsfall protein) may similarly mediate the uptake of surface layer protein A^+ lactic acid bacteria (31). Some pathogenic microorganisms appear to use receptors on M cells to aid host infection. The complement C5a receptor is expressed on the apical surface of M cells and aids the uptake of *Yersinia enterocolitica* to establish infection (32). Interactions between the type A 1 botulinum neurotoxin complex and GP2 on the M-cell surface have also

been shown to mediate the intestinal translocation of the toxin order to exert its toxic effects (33). M cells express the cellular isoform of the prion protein, PrP^C, on their apical surfaces (26, 34). Data suggest that the pathogenic Gram-negative bacterium *Brucella abortus* utilizes the PrP^C on the M-cell surface as an uptake receptor to enter Peyer's patches (26).

Whether the uptake and transcytosis of prions across the gut epithelium into Peyer's patches in order to establish infection predominantly occurs via constitutive sampling of the lumenal contents, or via binding to specific receptors such as PrP^C, is not known. Treatments that impede the early accumulation prions within the GALT can impede their spread to the brain and reduce disease susceptibility (4, 13, 16, 18). Thus the identification of the molecular factors that facilitate the uptake of prions into the GALT will help the design of novel intervention targets, and enhance our understanding of the factors that influence the risk of infection. Therefore, in the current study transgenic mice were created in which *Prnp* expression (encoding PrP^C) was specifically ablated in epithelial cells throughout the lining of the small intestine. These mice were then used to determine whether the absence of PrP^C expression in the epithelium lining the small intestine influences oral prion disease susceptibility and the early replication of prions in the GALT.

RESULTS

Conditional ablation of *Prnp* throughout the small intestinal epithelium. The expression of Cre recombinase under the control of the rat *Cyp1a1* promoter element in *Cyp1a1*-Cre mice has been used in a series of studies to inducibly ablate the expression of *LoxP* site-flanked target genes in small intestinal progenitor cells and intestinal epithelial cells (IEC) following β-naphthoflavone (βNF) treatment (35-

37). The FANTOM5 project of the FANTOM consortium (38) has collated a large collection of cap analysis of gene expression (CAGE) data from multiple mouse tissues and cells (http://fantom.gsc.riken.jp/zenbu). We used this publicly available data resource to compare the expression of levels of *Cyp1a1*, *Gp2* and *Prnp* in multiple data sets derived from mouse FAE, M cells, lymphocytes and leukocytes, and brain-derived cells. This analysis confirmed that *Cyp1a1* and *Prnp* were also expressed highly in the FAE and in $GP2^{+}$ M cells (**Fig. 1**). However, *Cyp1a1* expression was absent in B cells, T cells and macrophages as well as brain-derived microglia, astrocytes and neurons (**Fig. 1**).

Here, *Cyp1a1*-Cre mice were crossed with $Prnp^{F/F}$ mice which carry a "floxed" *Prnp* gene (39) to enable the inducible ablation of *Prnp* specifically in IEC. Since the reliable detection of PrP^{C} in the gut epithelium by immunohistochemistry (IHC) is technically challenging, these mice were additionally crossed with $ROSA26^{F/F}$ reporter mice (40) to enable the cellular-specificity of the Cre-mediated gene ablation to be readily assessed by histological assessment of β-galactosidase (*LacZ*) expression. The resultant progeny *Cyp1a1*-Cre $ROSA26^{F/F}$ $Prnp^{F/F}$ mice were termed $Prnp^{\Delta IEC}$ mice, hereinafter.

Female $Prnp^{\Delta IEC}$ mice were treated with βNF (or vehicle alone as a control) for five days to specifically ablate *Prnp* expression in IEC and tissues analyzed 14 days later. Whole-mount histological analysis showed *LacZ* expression indicative of efficient Cre-mediated gene recombination throughout the small and large intestines of βNF-treated $Prnp^{\Delta IEC}$ mice (**Fig. 2a**). Analysis of tissue sections showed strong *LacZ* expression in IEC and crypts throughout the small intestine (**Fig. 2c**). The Cre-mediated gene recombination in the small intestinal crypts of βNF-treated $Prnp^{\Delta IEC}$ mice was highly efficient (99.5% ± 1.1; **Fig. 2e**). In contrast, the Cre-mediated gene recombination in colonic crypts and IEC in the large intestine was

less efficient (64.1% ± 8.6; **Fig. 2f**) and presented as a mosaic pattern (**Fig. 2c**). No other cellular sites of Cre-mediated recombination were observed throughout the intestines of βNF-treated *Prnp*$^{\Delta IEC}$ mice. *LacZ* expression was absent within the submucosa (**Fig. 2c**), and also in the sub-epithelial dome and FDC-containing B cell-follicle regions of the GALT (**Fig. 2g**). As anticipated, no *LacZ* expression was detected throughout the small and large intestines of vehicle-treated *Prnp*$^{\Delta IEC}$ control mice (**Fig. 2b, d, e, f, h**). *LacZ* expression was also undetectable throughout the small and large intestines of untreated *Prnp*$^{\Delta IEC}$ control mice and βNF-treated *Prnp*$^{F/F}$ (Cre-deficient) control mice (**Fig. 2 e, f**). These data clearly demonstrate that Cre-mediated gene recombination is restricted to IEC in the small intestines of βNF-treated *Prnp*$^{\Delta IEC}$ mice.

Effect of IEC-restricted *Prnp*-ablation on prion accumulation in lymphoid tissues. To determine the effects of IEC-specific PrP^{C}-deficiency on oral prion disease pathogenesis, groups of female *Prnp*$^{\Delta IEC}$ mice were treated with βNF for five days to specifically ablate *Prnp* expression in IEC. Untreated *Prnp*$^{\Delta IEC}$ mice, vehicle-treated *Prnp*$^{\Delta IEC}$ mice and βNF-treated *Prnp*$^{F/F}$ (Cre-deficient) mice were used as controls. Fourteen days later 10 mice/group were subsequently orally exposed to ME7 scrapie prions and tissues collected at 70 days post-infection. The presence of the prion disease-specific, abnormal accumulations of PrP (referred to as PrP^{d}) which occur only in the tissues of affected animals was detected by IHC (4, 5, 11, 13, 16, 19, 41-43). However, since the IHC analysis cannot unequivocally discriminate between PrP^{Sc} and cellular PrP^{C}, paraffin-embedded tissue immunoblot analysis of adjacent membrane-bound sections was also used to confirm that these PrP^{d} aggregates contained prion disease-specific, relatively proteinase-K (PK)-resistant PrP^{Sc}. As anticipated, abundant PrP^{Sc} accumulations were detected in

association with FDC (CD21/35^{+} cells) in the Peyer's patches of control *Prnp*$^{\Delta IEC}$ mice (**Fig. 3a**, arrows, left-hand and middle columns). Abundant FDC-associated PrP^{Sc} accumulations were also detected in the Peyer's patches of βNF-treated *Prnp*$^{\Delta IEC}$ mice.

Consistent with the IHC data (**Fig. 3a**) high levels of prion infectivity were detected in the Peyer's patches of mice from each control group (median infectivity level 6.0-6.6 Log_{10} intracerebral [IC] infectious dose $[ID]_{50}$ units/g, *n* = 2-4 mice/group; **Fig 3b**). IEC-restricted *Prnp*-ablation did not influence the early accumulation of infectious prions within Peyer's patches as high levels of prion infectivity were also detected in tissues from βNF-treated *Prnp*$^{\Delta IEC}$ mice (median infectivity level 6.1 Log_{10} IC ID_{50} infectious units/g, *n* = 4 mice; **Fig 3b**).

Within weeks after oral exposure, high levels of ME7 scrapie prions first accumulate upon FDC in the Peyer's patches and are subsequently disseminated via the blood and lymph to most other lymphoid tissues including the MLN and spleen (4, 5, 11, 13, 16, 18, 19, 44). The levels of prion infectivity detected in the MLN and spleens from mice from each treatment and control group were also similar (**Fig. 3c & d**, respectively).

These data clearly show that IEC-restricted *Prnp*-ablation does not affect the early accumulation of orally-acquired prions within Peyer's patches or their subsequent dissemination to the MLN or spleen.

IEC-restricted *Prnp*-ablation does not influence oral prion disease susceptibility. Female *Prnp*$^{\Delta IEC}$ mice were treated with βNF for five days to ablate *Prnp* expression in IEC, and 14 days later subsequently orally exposed to ME7 scrapie prions. Untreated *Prnp*$^{\Delta IEC}$ mice, vehicle-treated *Prnp*$^{\Delta IEC}$ mice and βNF-treated *Prnp*$^{F/F}$ (Cre-deficient) mice were used as controls. As anticipated, all of the

orally-exposed untreated *Prnp*$^{\Delta IEC}$ (control) mice succumbed to clinical prion disease (mean survival time 307 ± 23 days; median 300 days, *n* = 10/10; **Table 1**). Furthermore, IEC-restricted *Prnp*-ablation did not affect disease duration (survival times) or susceptibility as all of the βNF-treated *Prnp*$^{\Delta IEC}$ mice also succumbed to clinical prion disease with similar survival times (mean 306 ± 11 days; median 306 days, *n* = 12/12, *P* = 0.673, One-way ANOVA with Dunnett's post-test; **Table 1**).

All the brains from the clinically-affected mice in each group displayed the characteristic spongiform pathology (vacuolation), PrP^{Sc} accumulation, astrogliosis and microgliosis which is associated with terminal infection with ME7 scrapie prions (**Fig. 4a&b**). The severity and distribution of the spongiform pathology was also similar in the brains of the clinically-affected mice from each group (**Fig. 4c**).

Together these data clearly show that efficient prion neuroinvasion after oral exposure occurs independently of PrP^{C} expression in IEC in the small intestine.

DISCUSSION

The initial transport of prions across the gut epithelium by M cells into small intestinal Peyer's patches is essential to establish efficient infection after oral exposure (13, 16). But whether the uptake and translocation of prions across the gut epithelium involves a specific receptor is uncertain. Treatments that prevent the initial replication of prions within the GALT impede the spread of prions to the brain and reduce disease susceptibility (4, 13, 16, 18). Thus the identification of the molecular factors that facilitate the uptake of prions into the GALT will help the design of novel intervention strategies, and enhance our understanding of the factors that influence the risk of infection. Small intestinal M cells express cellular PrP^{C} on their apical surfaces and this may be used by certain gastronintestinal

241 pathogens as an uptake receptor to infect Peyer's patches (26, 34). Independent
242 IHC-based tracing studies have suggested that orally-administered prion protein can
243 be transported across the gut epithelium of PrP^{C}-deficient mice (14, 17), but whether
244 the expression of PrP^{C} on IEC populations contributed to the establishment of host
245 infection had not been assessed. Data in the current study clearly show that prion
246 neuroinvasion after oral exposure occurs independently of PrP^{C} expression in small
247 intestinal IEC.

248 Orally-acquired prions replicate first in the small intestinal GALT and
249 subsequently spread to most other secondary lymphoid tissues including the large
250 intestinal GALT. Since oral prion disease susceptibility is substantially reduced in
251 the specific absence of the small intestinal GALT (11), this suggests that the early
252 replication of prions within Peyer's patches is essential to establish efficient host
253 infection after oral exposure. The small intestinal GALT also appear to be the
254 important early sites of prion replication in natural host species (45-47). Although
255 we observed highly efficient Cre-mediated gene recombination in intestinal crypts
256 and IEC throughout the small intestines of βNF-treated $Prnp^{\Delta IEC}$ mice, the efficiency
257 in the colon was less efficient and presented as a mosaic pattern (**Fig. 2c**) (35). The
258 less efficient *Prnp*-ablation in the large intestine was unlikely to have influenced oral
259 prion disease pathogenesis in the current study, as the large intestinal GALT such
260 as the colonic patches are not important early sites of prion replication and
261 neuroinvasion (11).

262 Despite the potentially widespread exposure of the UK population to BSE-
263 contaminated food in the 1980s, there have fortunately there have been much fewer
264 clinical cases of variant Creutzfeldt-Jakob disease in humans than the original
265 estimates suggested (48) (178 definite or probable cases, as of 4th May 2018; (49)).
266 This implies that additional factors could potentially influence an individual's

susceptibility to oral prion infection by enhancing or impeding the initial uptake of prions from the gut lumen. In support of this hypothesis we have shown that stimuli that increase the density of M cells in the gut epithelium also increase oral prion disease susceptibility approx 10 fold by enhancing the uptake of prions into Peyer's patches (16). The expression level of PrP^C in host cells such as neurones and FDC directly influences survival times in prion infected mice (43, 50-52). Acute mucosal inflammation following oral infection with *S*. Typhimurium or treatment with dextran sodium sulphate have each been shown to enhance PrP^C expression in the large intestine, implying the potential to enhance oral prion disease pathogenesis and susceptibility (53, 54). Conversely, PrP^C expression was reported to be down-regulated in the small intestines of mice treated with the nonsteroidal anti-inflammatory drug indomethacin, and coincided with a modest increase in survival time after oral exposure to ME7 scrapie prions (55). Although the cellular sites of PrP^C expression were not determined in the above studies, our data suggest that the magnitude of PrP^C expression in IEC throughout the small intestine is unlikely to be an important factor which influences the risk of oral prion disease susceptibility.

In sheep with natural scrapie (56) or orally exposed to BSE prions (57), prion accumulation is first detected in the palantine tonsils in addition to the Peyer's patches. Natural prion disease susceptible host species such as sheep and cervids also have highly developed olfactory systems which they use to detect food, select mates and sense predators. A series of experimental studies in rodents and sheep have shown that prion infections can be established via the nasal cavity (58, 59) (60). Thus it cannot be excluded that soil-bound prions might also be inhaled and infect the host as the animal forages for food. Although M cells are present in the epithelia covering the nasal-associated lymphoid tissue (61), studies in hamsters indicate that these prion uptake across the nasal epithelium occurs independently of M cells (62). Whether prion uptake across

the mucosal surfaces in the upper gastrointestinal and upper respiratory tracts of natural host species is also PrP^C-independent remains to be determined.

In conclusion, we show that oral prion disease neuroinvasion occurs independently of PrP^C expression in IEC in the small intestine. Whether prions exploit other receptors on the apical surfaces of M cells to establish host infection is uncertain. The specific targeting of vaccine antigens to M cells has been shown to be an effective method to induce protective antigen-specific mucosal immunity (63). Mucosal immunization has also been shown to provide promising protection against oral prion infections in mice (64) and white-tailed deer (65). Thus, a thorough understanding of the mechanisms that prions exploit to establish infection within the GALT may help to identify important factors which influence the disease susceptibility, or identify novel targets for prophylactic intervention.

MATERIALS AND METHODS

Mice. The following mouse strains were used in this study where indicated: *Cyp1a1*-Cre (35); $ROSA26^{F/F}$ reporter strain (40); $Prnp^{F/F}$ mice (strain $Prnp^{tm2Tuzi}$) which have *LoxP* sites flanking exon 3 of the *Prnp* gene (39). C57BL/Dk mice were also used where indicated. All mice were bred and maintained under SPF conditions. All studies and regulatory licences were approved by the Institute's ethics committee and carried out under the authority of a UK Home Office Project Licence. Prior to their use in experiments, the genotype of each mouse was confirmed by PCR analysis of tail DNA (**Table 2**).

β-naphthoflavone treatment. Where indicated, mice were given five daily intraperitoneal injections of β-naphthoflavone (80 mg/kg; Sigma-Aldritch, Poole, UK)

dissolved in corn oil (Sigma-Aldritch) and analyzed 14 days after the last injection or used in subsequent experiments. Where indicated, some mice received either corn oil alone (vehicle) or no treatment as controls.

Histological assessment of *LacZ* expression. Tissues were first immersed in *LacZ* fixative [PBS (pH 7.4) containing 2% paraformaldehyde, 0.2% gluteraldehyde, 0.02%
Nonidet P40, 0.01% sodium deoxycholate, 5 mM EGTA, 2 mM $MgCl_2$] and washed in *LacZ* wash buffer [PBS (pH 7.4) containing 0.02% Nonidet P40, 0.01% sodium deoxycholate, 2 mM $MgCL_2$]. Tissues were subsequently incubated in 15% (wt/vol) sucrose in PBS overnight followed by a further overnight incubation in 30% (wt/vol) sucrose in PBS and embedded in Tissue-Tek OCT compound (Bayer PLC, Newbury, UK). Serial sections (thickness 8 mm) were cut on cryostat and stained overnight at with *LacZ* staining solution (Glycosynth, Warrington, UK). Staining reaction was stopped by washing in *LacZ* wash buffer followed by distilled water. Sections were counterstained with nuclear fast red (Vector Laboratories, Peterborough, UK). Intestinal whole-mounts were prepared luminal side up as described previously (66), and fixed in ice-cold 2% formaldehyde/0.2% glutaraldehyde in PBS (pH 7.4) for 1 h before overnight incubation in *LacZ* staining solution.

Prion exposure and disease monitoring. For oral exposure, mice were fed individual food pellets dosed with 50 µl of a 1.0 % (w/v) dilution of scrapie brain homogenate (containing approximately 4.6 Log_{10} IC ID_{50} units) prepared from mice terminally-affected with ME7 scrapie prions according to our standard protocol (11, 16, 19). During the dosing period mice were individually housed in bedding- and

345 food-free cages with water provided *ad libitum*. A single prion-dosed food pellet was
346 then placed in the cage. The mice were returned to their original cages (with
347 bedding and food *ad libitum*) as soon as the food pellet was observed to have been
348 completely ingested. The use of bedding- and additional food-free cages ensured
349 easy monitoring of consumption of the prion-contaminated food pellet. Following
350 prion exposure, mice were coded and assessed weekly for signs of clinical disease
351 and culled at a standard clinical endpoint. The clinical endpoint of disease was
352 determined by rating the severity of clinical signs of prion disease exhibited by the
353 mice. Mice were clinically scored as “unaffected”, “possibly affected” and “definitely
354 affected” using standard criteria which typically present in mice terminal ME7
355 scrapie prion disease. Clinical signs following infection with the ME7 scrapie prions
356 may include: weight-loss, starry coat, hunched, jumpy behaviour (at early onset)
357 progressing to limited movement, upright tail, wet genitals, decreased awareness,
358 discharge from eyes/blinking eyes, ataxia of hind legs. The clinical endpoint of
359 disease was defined in one of the following ways: i) the day on which a mouse
360 received a second consecutive “definite” rating; ii) the day on which a mouse
361 received a third “definite” rating within four consecutive weeks; iii) the day on which
362 a mouse was culled in extremis. Prion diagnosis was confirmed by histopathological
363 assessment of the magnitude of the spongiform pathology (vacuolation) in nine
364 distinct grey-matter regions of the brain as described (67).

365 For bioassay of prion infectivity, individual tissues were prepared as 10 %
366 (w/v) homogenates and 20 µl was injected IC into each of 4 recipient C57BL/Dk
367 indicator mice. The prion infectivity titre in each sample was determined from the
368 mean incubation period in the indicator mice, by reference to a dose/incubation
369 period response curve for ME7 scrapie-infected spleen tissue serially titrated in
370 C57BL/Dk indicator mice (68).

371

372 **Immunohistochemisty.** For the detection of disease-specific PrP (PrP^d) in
373 intestines and brains, tissues were fixed in periodate-lysine-paraformaldehyde
374 fixative and embedded in paraffin wax. Sections (thickness, 6 µm) were
375 deparaffinised, and pre-treated to enhance the detection of PrP^d by hydrated
376 autoclaving (15 min, 121ºC, hydration) and subsequent immersion in formic acid
377 (98%) for 5 min. Sections were then immunostained with 1B3 PrP-specific pAb. For
378 the detection of FDC in intestines deparaffinised sections were first pre-treated with
379 Target Retrieval Solution (DAKO) and subsequently immunostained with anti-
380 CD21/35 (clone 7G6, BD Biosciences). Paraffin-embedded tissue immunoblot
381 analysis was used to confirm that the PrP^d detected by immunohistochemistry was
382 proteinase K-resistant PrP^{Sc} (69). Membranes were subsequently immunostained
383 with 1B3 PrP-specific pAb.

384 For the detection of astrocytes, brain sections were immunostained with anti-
385 glial fibrillary acidic protein (GFAP; DAKO, Ely, UK), and to detect microglia sections
386 were immunostained with anti-ionized calcium-binding adaptor molecule 1 (Iba-1;
387 Wako Chemicals GmbH, Neuss, Germany).

388 Following the addition of primary antibodies, biotin-conjugated species-
389 specific secondary antibodies (Stratech, Soham, UK) were applied and
390 immunolabelling was revealed using either alkaline phoshatase-conjugated to the
391 avidin-biotin complex (Vector Laboratories, Peterborough, UK) and visualized using
392 Vector Red (Vector Red), or HRP-conjugated to the avidin-biotin complex (Vector
393 Laboratories) and visualized with DAB (Sigma). Sections were counterstained with
394 haematoxylin to distinguish cell nuclei.

395

396 **Immunoblot detection of PrP^{Sc}**

Brain homogenates (10% weight/volume) were prepared in NP40 lysis buffer (1% NP40, 0.5% sodium deoxycholate, 150 mM NaCl, 50 mM TrisHCL [pH 7.5]) and incubated at 37°C for 1 h with 20 µg/ml PK. Digestions were halted by addition of 1 mM phenylmethylsulfonyl fluoride. Samples were then subjected to electrophoresis through 12% Tris-glycine polyacrylamide gels (Nupage, Life Technologies) and transferred to PVDF membranes by semi-dry blotting. PrP was detected using anti-mouse PrP-specific mAb 7A12 (70) followed by horseradish peroxidase-conjugated goat anti-mouse antibody (Jackson Immunoresearch) and visualised chemiluminescence (BM Chemiluminescent substrate kit, Roche, Burgess Hill, UK).

Statistical analyses. Unless indicated otherwise, data are presented as mean ± SD and significant differences between groups were sought by Student's *t*-test. Values of $P < 0.05$ were accepted as significant.

ACKNOWLEDGEMENTS

The authors would like to dedicate this paper to Professor Alan Clarke (1963-2015) in recognition of his inspiration and support in this study. We also thank Nadia Tuzi, Dorothy Kisielewski, Rebecca Greenan, Simon Cumming, Val Thomson, Kris Hogan and the Pathology Services Group (University of Edinburgh, UK) for excellent technical support, and Abigail Diack (University of Edinburgh) for helpful discussion.

This work was supported by project funding from the Department of Health (PR-IP-0807-0070161) and Institute Strategic Programme Grant funding from the Biotechnology and Biological Sciences Research Council (grant numbers BBS/E/D/05241339, BBS/E/D/20251968 and BBS/E/D/20002174).

FIG 1 *Cyp1a1* is expressed in the follicle-associated epithelium and in M cells in the small intestine. Comparison of *Cyp1a1*, *Prnp* and *Gp2* mRNA expression in individual cell populations in deep cap analysis of gene expression (CAGE) sequence data from the FANTOM5 project of the FANTOM consortium (38). Each bar shows the relative expression level of each gene per million reads in each sample; RLE normalized tags/million). The blue hatched box highlights the small intestine-derived glycoprotein 2-expressing (GP2+) M-cell and the follicle-associated epithelium datasets. The red hatched box highlights the brain-derived datasets.

FIG 2 Cre-mediated gene recombination is restricted to IEC in the small intestines of βNF-treated $Prnp^{\Delta IEC}$ mice. Female $Prnp^{\Delta IEC}$ mice were treated with β-naphthoflavone (βNF) for five days to specifically ablate *Prnp* expression in intestinal epithelial cells and tissues analyzed 14 days later. $Prnp^{\Delta IEC}$ mice treated with vehicle alone (Veh.) were used as controls. (A, B) Whole-mount histological analysis of *LacZ* expression (blue) in the intestines of (A) βNF-treated $Prnp^{\Delta IEC}$ mice or (B) vehicle-treated $Prnp^{\Delta IEC}$ control mice. S, small intestine. L, large intestine. (C, D) Histological analysis of *LacZ* expression (blue) in IEC and crypts in the intestines of (C) βNF-treated $Prnp^{\Delta IEC}$ mice or (D) vehicle-treated $Prnp^{\Delta IEC}$ control mice. Sections were counterstained with nuclear fast red to detect cell nuclei (red). SM, submucosa. (E, F) Comparison of the % *LacZ*-expressing crypts in (E) the small and (F) large intestines, of βNF-treated $Prnp^{F/F}$ mice control mice. Untreated $Prnp^{\Delta IEC}$ mice, vehicle-treated $Prnp^{\Delta IEC}$ mice and βNF-treated $Prnp^{F/F}$ mice were used as controls. Data represent mean % *LacZ*-expressing crypts/mouse (n = 5 mice/group, 50-105 crypts/mouse). (G, H) Histological analysis of *LacZ* expression (blue) in the Peyer's patches and colonic patches of (G) βNF-treated $Prnp^{\Delta IEC}$ mice or (H) vehicle-treated $Prnp^{\Delta IEC}$ control mice.

449

450 **FIG 3** Effect of intestinal epithelial cell-restricted *Prnp*-ablation on prion
451 accumulation in lymphoid tissues. Female $Prnp^{\Delta IEC}$ mice were treated with β-
452 naphthoflavone (βNF) for five days to specifically ablate *Prnp* expression in intestinal
453 epithelial cells. Untreated $Prnp^{\Delta IEC}$ mice and $Prnp^{\Delta IEC}$ mice treated with vehicle
454 alone (Veh.) were used as controls. Fourteen days later the mice were orally
455 exposed to ME7 scrapie prions and Peyer's patches, mesenteric lymph nodes
456 (MLN) and spleens collected at 70 days post infection. (A) Immunohistochemical
457 analysis revealed high levels of disease-specific PrP (PrP^d, red, middle row, arrows)
458 were detected in association with FDC ($CD21/35^+$ cells, red, upper row) in Peyer's
459 patches from mice from each group. Sections were counterstained with
460 haematoxylin to detect cell nuclei (blue). Analysis of adjacent sections by paraffin-
461 embedded tissue immunoblot analysis confirmed the presence of prion-specific PK-
462 resistant PrP^{Sc} (blue/black). Data representative of tissues from 6 mice/group. (B,
463 C, D) Prion infectivity levels were assayed in (B) Peyer's patches, (C) MLN and (D)
464 spleens from mice from each group collected at 70 days post infection. Prion
465 infectivity titres (log_{10} IC ID_{50}/g tissue) were determined by injection of tissue
466 homogenates into groups of C57BL/Dk indicator mice (*n* = 4 recipient mice/tissue).
467 Each symbol represents data derived from an individual tissue. Red line, median
468 prion infectivity titre for groups in which all samples contained >1 log_{10} IC ID_{50}/g
469 tissue. Data below the broken horizontal line indicate disease incidence in the
470 recipient mice <100% and considered to contain trace levels of prion infectivity.

471

472 **FIG 4.** Intestinal epithelial cell-restricted *Prnp*-ablation does not influence
473 development of the histopathological signs prion disease in the brains of clinically
474 affected mice. Female $Prnp^{\Delta IEC}$ mice were treated with β-naphthoflavone (βNF) for

five days to specifically ablate *Prnp* expression in intestinal epithelial cells. Untreated $Prnp^{\Delta IEC}$ mice and $Prnp^{\Delta IEC}$ mice treated with vehicle alone (Veh.) were used as controls. Fourteen days later the mice were orally exposed to ME7 scrapie prions and culled when they succumbed to clinical prion disease. (A) High levels of spongiform pathology (H&E), heavy accumulations of disease-specific PrP, (PrP^{d}, brown), reactive astrocytes expressing GFAP (brown) and active microglia expressing IBA1 (brown) were detected in the brains of all orally-exposed mice with clinical prion disease. Clin., clinical prion disease status; pos., clinically positive; individual survival times are shown (dpi, days post infection). Sections were counterstained with haematoxylin to detect cell nuclei (blue). (B) Immunoblot analysis of brain tissue homogenates confirmed the presence of high levels of prion-specific, relatively proteinase K (PK)-resistant PrP^{Sc} within the brains of the clinically-affected mice from each group. Samples were treated in the presence (+) or absence (-) of PK before electrophoresis. After PK treatment, a typical three-band pattern was observed between molecular mass value of 20–30 kDa, representing unglycosylated, monoglycosylated, and diglycosylated isomers of PrP (in order of increasing molecular mass). (C) The severity and distribution of the spongiform pathology (vacuolation) within each brain was scored on a scale of 1–5 in nine grey matter areas: G1, dorsal medulla; G2, cerebellar cortex; G3, superior colliculus; G4, hypothalamus; G5, thalamus; G6, hippocampus; G7, septum; G8, retrosplenial and adjacent motor cortex; G9, cingulate and adjacent motor cortex. Each point represents the mean vacuolation score ± SD (*n* = 10-12 mice/group).

REFERENCES

1. **Bruce ME, Will RG, Ironside JW, McConnell I, Drummond D, Suttie A, McCardle L, Chree A, Hope J, Birkett C, Cousens S, Fraser H, Bostock CJ.** 1997. Transmissions to mice indicate that 'new variant' CJD is caused by the BSE agent. Nature **389:**498-501.
2. **Legname G, Baskakov IV, Nguyen H-OB, Riesner D, Cohen FE, DeArmond SJ, Prusiner SB.** 2004. Synthetic mammalian prions. Science **305:**673-676.
3. **Manson JC, Clarke AR, Hooper ML, Aitchison L, McConnell I, Hope J.** 1994. 129/Ola mice carrying a null mutation in PrP that abolishes mRNA production are developmentally normal. Molecular Neurobiology **8:**121-127.
4. **Mabbott NA, Young J, McConnell I, Bruce ME.** 2003. Follicular dendritic cell dedifferentiation by treatment with an inhibitor of the lymphotoxin pathway dramatically reduces scrapie susceptibility. Journal of Virology **77:**6845-6854.
5. **Glaysher BR, Mabbott NA.** 2007. Role of the GALT in scrapie agent neuroinvasion from the intestine. Journal of Immunology **178:**3757-3766.
6. **Andreoletti O, Berthon P, Marc D, Sarradin P, Grosclaude J, van Keulen L, Schelcher F, Elsen J-M, Lantier F.** 2000. Early accumulation of PrP^{Sc} in gut-associated lymphoid and nervous tissues of susceptible sheep from a Romanov flock with natural scrapie. Journal of General Virology **81:**3115-3126.
7. **Sigurdson CJ, Williams ES, Miller MW, Spraker TR, O'Rourke KI, Hoover EA.** 1999. Oral transmission and early lymphoid tropism of chronic wasting disease PrP^{res} in mule deer fawns (*Odocoileus hemionus*). Journal of General Virology **80:**2757-2764.
8. **Hilton D, Fathers E, Edwards P, Ironside J, Zajicek J.** 1998. Prion immunoreactivity in appendix before clinical onset of variant Creutzfeldt-Jakob disease. Lancet **352:**703-704.
9. **Prinz M, Huber G, Macpherson AJS, Heppner FL, Glatzel M, Eugster H-P, Wagner N, Aguzzi A.** 2003. Oral prion infection requires normal numbers of Peyer's patches but not of enteric lymphocytes. American Journal of Pathology **162:**1103-1111.
10. **Horiuchi M, Furuoka H, Kitamura N, Shinagawa M.** 2006. Alymphoplasia mice are resistant to prion infection via oral route. Japanese Journal of Veterinary Research **53:**149-157.
11. **Donaldson DS, Else KJ, Mabbott NA.** 2015. The gut-associated lymphoid tissues in the small intestine, not the large intestine, play a major role in oral prion disease pathogenesis. Journal of Virology **15:**9532-9547.
12. **Heppner FL, Christ AD, Klein MA, Prinz M, Fried M, Kraehenbuhl J-P, Aguzzi A.** 2001. Transepithelial prion transport by M cells. Nature Medicine **7:**976-977.
13. **Donaldson DS, Kobayashi A, Ohno H, Yagita H, Williams IR, Mabbott NA.** 2012. M cell depletion blocks oral prion disease pathogenesis. Mucosal Immunology **5:**216-225.
14. **Takakura I, Miyazawa K, Kanaya T, Itani W, Watanabe K, Ohwada S, Watanabe H, Hondo T, Rose MT, Mori T, Sakaguchi S, Nishida N, Katamine S, Yamaguchi T, Aso H.** 2011. Orally administered prion protein is incorporated by M cells and spreads to lymphoid tissues with macrophages in prion protein knockout mice. American Journal of Pathology **179:**1301-1309.
15. **Miyazawa K, Kanaya T, Takakura I, Tanaka S, Hondo T, Watanabe H, Rose MT, Kitazawa H, Yamaguchi T, Katamine S, Nishida N, Aso H.** 2010. Transcytosis of murine-adapted bovine spongiform encephalopathy agents in an in vitro bovine M cell model. Journal of Virology **84:**12285-12291.

16. **Donaldson DS, Sehgal A, Rios D, Williams IR, Mabbott NA.** 2016. Increased abundance of M cells in the gut epithelium dramatically enhances oral prion disease susceptibility. PLoS Pathogens **12:**e1006075.
17. **Kujala P, Raymond C, Romeijn M, Godsave SF, van Kasteren SI, H. W, Prusiner SB, Mabbott NA, Peters PJ.** 2011. Prion uptake in the gut: identification of the first uptake and replication sites. PLoS Pathogens **7:**e1002449.
18. **Raymond CR, Aucouturier P, Mabbott NA.** 2007. *In vivo* depletion of $CD11c^{+}$ cells impairs scrapie agent neuroinvasion from the intestine. Journal of Immunology **179:**7758-7766.
19. **Bradford BM, Reizis B, Mabbott NA.** 2017. Oral prion disease pathogenesis is impeded in the specific absence of CXCR5-expressing dendritic cells. Journal of Virology **91:**e00124-00117.
20. **McCulloch L, Brown KL, Mabbott NA.** 2013. Ablation of the cellular prion protein, PrP^{C}, specifcally on follicular dendritic cells has no effect on their maturation or function. Immunology **138:**246-257.
21. **Beekes M, McBride PA.** 2007. The spread of prions through the body in naturally acquired transmissible spongiform encephalopathies. FEBS Journal **274:**588-605.
22. **Mabbott NA, Donaldson DS, Ohno H, Williams IR, Mahajan A.** 2013. Microfold (M) cells: important immunosurveillance posts in the intestinal epithelium. Mucosal Immunology **6:**666-677.
23. **Hase K, Kawano K, Nochi T, Pontes GS, Fukuda S, Ebisawa M, Kadokura K, Tobe T, Fujimura Y, Kawano S, Yabashi A, Waguri S, Nakato G, Kimura S, Murakami T, Iimura M, Hamura K, Fukuoka S-I, Lowe AW, Itoh K, Kiyono H, Ohno H.** 2009. Uptake through glycoprotein 2 of $FimH^{+}$ bacteria by M cells initiates mucosal immune responses. Nature **462:**226-231.
24. **Kanaya T, Hase K, Takahashi D, Fukuda S, Hoshino K, Sasaki I, Hemmi H, Knoop KA, Kumar N, Sato M, Katsuno T, Yokosuka O, Toyooka K, Nakai K, Sakamoto A, Kitahara Y, Jinnohara T, McSorley SJ, Kaisho T, Williams IR, Ohno H.** 2012. The Ets transcription factor Spi-B is essential for the differentiation of intestinal microfold cells. Nature Immunology **13:**729-736.
25. **Rios D, Wood MB, Li J, Chassaing B, Gewirtz AT, Williams IR.** 2016. Antigen sampling by intestinal M cells is the principal pathway initiating mucosal IgA production to commensal enteric bacteria. Mucosal Immunology **9:**907-916.
26. **Nakato G, Hase K, Suzuki M, Kimura M, Ato M, Hanazato M, Tobiume M, Horiuchi M, Atarashi R, Nishida N, Watarai H, Imaoka K, Ohno H.** 2012. Cutting edge: *Brucella abortus* exploits a cellular prion protein on intestinal M cells as an invasive receptor. Journal of Immunology **189:**1540-1544.
27. **Tahoun A, Mahajan S, Paxton E, Malterer G, Donaldson DS, Wang D, Tan A, Gillespie TL, O'Shea M, Rose A, Shaw DJ, Gally DL, Lengeling A, Mabbott NA, Haas J, Mahajan A.** 2012. Salmonella transforms follicle-associated epithelial cells into M cells to promote intestinal invasion. Cell Host & Microbe **12:**645-666.
28. **Westphal S, Lugering A, von Wedel J, von Eiff C, Maaser C, Spahn T, Heusipp G, Schmidt MA, Herbst H, Williams IR, Domschke W, Kucharzik T.** 2008. Resistance of chemokine receptor 6-deficient mice to *Yersinia enterocolitica* infection: evidence on defective M-cell formation *in vivo*. American Journal of Pathology **172:**671-680.
29. **Kolawole AO, Gonzalez-Hernandez MB, Turula H, Yu C, Elftman MD, Wobus CE.** 2015. Oral norovirus infection is blocked in mice lacking Peyer's patches and mature M cells. Journal of Virology **90:**1499-1506.
30. **Gonzalez-Hernandez MB, Liu T, Payne HC, Stencel-Baerenwald JE, Ikizler M, Yagita H, Dermody TS, Williams IR, Wobus CE.** 2014. Efficient norovirus and

reovirus replication in the mouse intestine requires microfold (M) cells. Journal of Virology **88:**6934-6943.

31. **Yanagihara S, Kanaya T, Fukuda S, Nakato G, Hanazato M, Wu XR, Yamamoto N, Ohno H.** 2017. Uromodulin-SlpA binding dictates *Lactobacillus acidophilus* uptake by intestinal M cells. International Immunology **29:**357-363.
32. **Kim S-H, Jang Y-S.** 2017. *Yersinia enterocolitica* epxloits signal crosstalk between complement C5a receptor and Toll-like receptor 1/2 to avoid the bacterial clearance in M cells. Immune Network **17:**228-236.
33. **Matsumura T, Sugawara Y, Yutani M, Amatsu S, Yagita H, Kohda T, Fukuoka S-I, Nakamura Y, Fukuda S, Hase K, Ohno H, Fujinaga Y.** 2015. Botulinum toxin A complex exploits intestinal M cells to enter the host and exert neurotoxicity. Nature Communications **6:**6255.
34. **Nakato G, Fukuda S, Hase K, Goitsuka R, Cooper MD, Ohno H.** 2009. New approach for M-cell-specific molecules by screening comprehensive transcriptome analysis. DNA Research **16:**227-235.
35. **Ireland H, Kemp R, Houghton C, Howard L, Clarke AR, Sansom OJ, Winton DJ.** 2004. Inducible Cre-mediated control of gene expression in the murine gastrointestinal tract: effect of loss of β-catenin. Gastroenterology **126:**1236-1246.
36. **Gonneaud A, Turgeon N, Boudreau F, Perrault N, Rivard N, Asselin C.** 2016. Distinct roles for intestinal epithelial cell-specific Hdac1 and Hdac2 in the regulation of murine intestinal homeostasis. Journal of Cellular Physiology **231:**436-448.
37. **Asano J, Sato T, Ichinose S, Kajita M, Onai N, Shimizu S, Ohteki T.** 2017. Intrinsic autophagy is required for the maintenance of intestinal stem cells and for irradiation-induced intestinal regeneration Cell Reports **20:**1050-1060.
38. **(DGT) FCatRPaC, Forrest AR.** 2014. A promoter-level mammalian expression atlas. Nature **507:**462-470.
39. **Tuzi NL, Clarke AR, Bradford B, Aitchison L, Thomson V, Manson JC.** 2004. Cre-loxP mediated control of PrP to study transmissible spongiform encephalopathy diseases. Genesis **40:**1-6.
40. **Mao X, Fujiwara Y, Orkin SH.** 1999. Improved reporter strain for monitoring Cre recombinase-mediated DNA excisions in mice. Proceedings of the National Academy of Sciences, USA **96:**5037-5042.
41. **McBride P, Eikelenboom P, Kraal G, Fraser H, Bruce ME.** 1992. PrP protein is associated with follicular dendritic cells of spleens and lymph nodes in uninfected and scrapie-infected mice. Journal of Pathology **168:**413-418.
42. **Mabbott NA, Mackay F, Minns F, Bruce ME.** 2000. Temporary inactivation of follicular dendritic cells delays neuroinvasion of scrapie. Nature Medicine **6:**719-720.
43. **Brown KL, Stewart K, Ritchie D, Mabbott NA, Williams A, Fraser H, Morrison WI, Bruce ME.** 1999. Scrapie replication in lymphoid tissues depends on PrP-expressing follicular dendritic cells. Nature Medicine **5:**1308-1312.
44. **Mok SW, Proia RL, Brinkmann V, Mabbott NA.** 2012. B cell-specific S1PR1 deficiency blocks prion dissemination between secondary lymphoid organs. Journal of Immunology **188:**5032-5040.
45. **van Keulen LJ, Schreuder BE, Vromans ME, Langeveld JP, Smits MA.** 2000. Pathogenesis of natural scrapie in sheep. Archives of Virology Supplementum **16:**57-71.
46. **Gonzalez L, Martin S, Siso S, Konold T, Ortiz-Pelaez A, Phelan L, Goldmann W, Stewart P, Saunders G, Windl O, Jeffrey M, Hawkins SAC, Dawson M, Hope J.** 2009. High prevalence of scrapie in a dairy goat herd: tissue distribution of disease-associated PrP and effect of *PRNP* genotype and age. Veterinary Research **40:**65.

47. **Thomsen BV, Schneider DA, O'Rourke KI, Gidlewski T, McLane J, Allen RW, mcIsaac AA, Mitchell GB, Keane DP, Spraker TR, Balachandran A.** 2012. Diagnostic accuracy of rectal mucosa biopsy testing for chronic wasting disease within white-tailed deer (*Odocoileus virginianus*) herds in North America: effects of age, sex, polymorphism at *PRNP* codon 96, and disease progression. Journal of Veterinary Diagnostics and Intestigation **24:**878-887.

48. **Diack AB, Head MW, McCutcheon S, Boyle A, Knight R, Ironside JW, Manson JC, Will RG.** 2014. Variant CJD. 18 years of research and surveillance. Prion **2014:**286-295.

49. The Nationa CJD Research and Surveillance Unit. www.cjd.ed.ac.uk. Accessed 4/5/18.

50. **Manson JC, Clarke AR, McBride PA, McConnell I, Hope J.** 1994. PrP gene dosage determines the timing but not the final intensity or distribution of lesions in scrapie pathology. Neurodegeneration **3:**331-340.

51. **Klein MA, Frigg R, Raeber AJ, Flechsig E, Hegyi I, Zinkernagel RM, Weissmann C, Aguzzi A.** 1998. PrP expression in B lymphocytes is not required for prion neuroinvasion. Nature Medicine **4:**1429-1433.

52. **McCulloch L, Brown KL, Bradford BM, Hopkins J, Bailey M, Rajewsky K, Manson JC, Mabbott NA.** 2011. Follicular dendritic cell-specific prion protein (PrP^{C}) expression alone is sufficient to sustain prion infection in the spleen. PLoS Pathogens **7:**e1002402.

53. **Martin GR, Keenan CM, Sharkey KA, Jirik FR.** 2011. Endogenous prion protein attenuates experimentally induced colitis. American Journal of Pathology **179:**2290-2301.

54. **Sigurdson CJ, Heikenwalder M, Manco G, Barthel M, Schwarz P, Stecher B, Krautler NJ, Hardt W-D, Seifert B, MacPherson AJS, Corthesy I, Aguzzi A.** 2009. Bacterial colitis increases susceptibility to oral prion pathogenesis. Journal of Infectious Diseases **199:**243-252.

55. **Martin GR, Sharkey KA, Jirik FR.** 2015. Orally administered indomethacin acutely reduces cellular prion protein in the small intestine and modest increases survival of mice exposed to infectious prions. Scandinavian Journal of Gastroenterology **50:**542-549.

56. **van Keulen LJM, Vromans MEW, van Zijderveld FG.** 2002. Ealry and late pathogenesis of natural scrapie infection in sheep. APMIS **110:**23-32.

57. **Van Keulen LJM, Vromans MEW, Dolstra CH, Bossers A, van Zijderveld FG.** 2008. Pathogenesis of bovine spongiform encephalopathy in sheep. Archives of Virology **153:**445-453.

58. **Kincaid AE, Bartz JC.** 2007. The nasal cavity is a route for prion infection in hamsters. Journal of Virology **81:**4482-4491.

59. **Hamir AN, Kunkle RA, Richt JA, MIller JM, Greenlee JJ.** 2008. Experimental transmission of US scrapie agent by nasal, peritoneal, and conjuctival routes to genetically susceptible sheep. Veterinary Pathology **45:**7-11.

60. **Denkers ND, Seelig DM, Telling GC, Hoover EA.** 2010. Aerosol and nasal transmission of chronic wasting disease in cervidized mice. Journal of General Virology **91:**1651-1658.

61. **Mutoh M, Kimura S, Takashi-Iwanaga H, Hisamoto M, Iwanaga T, Iida J.** 2016. RANKL regulates differentiation of microfold cells in mouse nasopharynx-associated lymphoid tissue (NALT). Cell and Tissue Research **364:**175-184.

62. **Kincaid AE, Ayers JI, Bartz JC.** 2016. Specificity, size and frequency of spaces that characterize the mechanism of bulk transepithelial transport of prions in the nasal cavities of hamsters and mice. Journal of Virology **90:**8293-8301.

63. **Shima H, Watanabe T, Fukuda S, Fukuoka S-I, Ohara O, Ohno H.** 2014. A novel vaccine targeting Peyer's patch M cells induces protective antigen-specific IgA responses. International Immunology **26:**619-625.

64. **Goñi F, Chablagoity JA, Prelli F, Schreiber F, Scholtzova H, Chung E, Kascsak R, Brown DR, Sigurdsson EM, Wisniewski T.** 2008. High titres of mucosal and systemic anti-PrP antibodies abrogates oral prion infection in mucosal vaccinated mice. Neuroscience **153:**679-686.

65. **Goñi F, Mathiason CK, Yim L, Wong K, Hayes-Klug J, Nalls A, Peyser D, Estevez V, Denkers N, Xu J, Osborn DA, Miller KV, Warren RJ, Brown DR, Chabalgoity JA, Hoover EA, Wisniewski T.** 2015. Mucosal immunization with an attenuated Salmonella vaccine partially protects white-tailed deer from chronic wasting disease. Vaccine **33:**726-733.

66. **Winton DJ, Ponder BAJ.** 1990. Stem cell organisation in mouse small intestine. Proceedings of the Royal Society of London B Biological Sciences **241:**13-18.

67. **Fraser H, Dickinson AG.** 1968. The sequential development of the brain lesions of scrapie in three strains of mice. Journal of Comparative Pathology **78:**301-311.

68. **Brown KL, Wathne GJ, Sales J, Bruce ME, Mabbott NA.** 2009. The effects of host age on follicular dendritic cell status dramatically impair scrapie agent neuroinvasion in aged mice. Journal of Immunology **183:**5199-5207.

69. **Schulz-Schaeffer WJ, Tschoke S, Kranefuss N, Drose W, Hause-Reitner D, Giese A, Groschup MH, Kretzschmar HA.** 2000. The paraffin-embedded tissue blot detects PrP^{sc} early in the incubation time in prion diseases. American Journal of Pathology **156:**51-56.

70. **Yin S, Pham N, Yu S, Li C, Wong P, Chang B, Kang S-C, Biasini E, Tien P, Harris DA, Sy M-S.** 2007. Human prion proteins with pathogenic mutations share common conformational changes resulting in enhanced binding to glycosaminoglycans. Proceedings of the National Academy of Sciences, USA **104:**7546-7551.

TABLE 1 *Prnp*-deficiency in the gut epithelium does not influence oral prion disease susceptibility

Mouse model[a]	Mean survival times (days±SD)[b,c]	Median survival times (days)	Clinical disease[d]	Histopathological signs of prion disease in the brain[e]
$Prnp^{\Delta IEC}$	307 ± 23	300	10/10	10/10
$Prnp^{\Delta IEC}$ + Veh.	303 ± 12	303	10/10	10/10
$Prnp^{\Delta IEC}$ + βNF	308 ± 11	306	12/12	12/12
$Prnp^{F/F}$ + βNF	313 ± 19	305	9/9	9/9

[a] Where indicated, mice were given daily IP injections with β-napthoflavone (βNF) or corn oil (Vehicle control, Veh.) for 5 days. Mice were orally exposed to ME7 scrapie prions 14 days after the last treatment.

[b] Duration from time of injection with prions to cull at clinical end-point.

[c] No statistical differences in survival times were observed between groups (*P*=0.673; One-way ANOVA with Dunnett's post-test.

[d] Incidence = no. animals displaying clinical signs of prion disease/no. animals tested.

[e] Incidence = no. animals with histopathological signs of prion disease in the brain (spongiform pathology)/no. animals tested.

TABLE 2 PCR primers used to confirm mouse genotypes

Allele	Details	Primer sequence	Product size/s (bp)
Cre	Fwd	CGAGTGATGAGGTTCGCAAGAACC	786
	Rev	GCTAAGTGCCTTCTCTACACCTGC	
LacZ	Fwd	TACCACAGCGGATGGTTCGG	300
	Rev	GTGGTGGTTATGCCGATCGC	
Prnp^{flox}	1	AATGGTTAAACTTTCGTTAAGGAT	Recombined *Prnp*^{F} 344
	2	GCCGACATCAGTCCACATAG	*Prnp*^{F} 210
	3	GGTTGACGCCATGACTTTC	*Prnp*$^{+}$ 167
Prnp^{+}	Fwd	TCATCCCACGATCAGGAAGATGAG	600
	Rev	ATGGCGAACCTTGGCTACTGGCTG	

Fwd, forward primer; Rev, reverse primer; Recombined *Prnp*^{F}, Cre-mediated DNA recombined allele

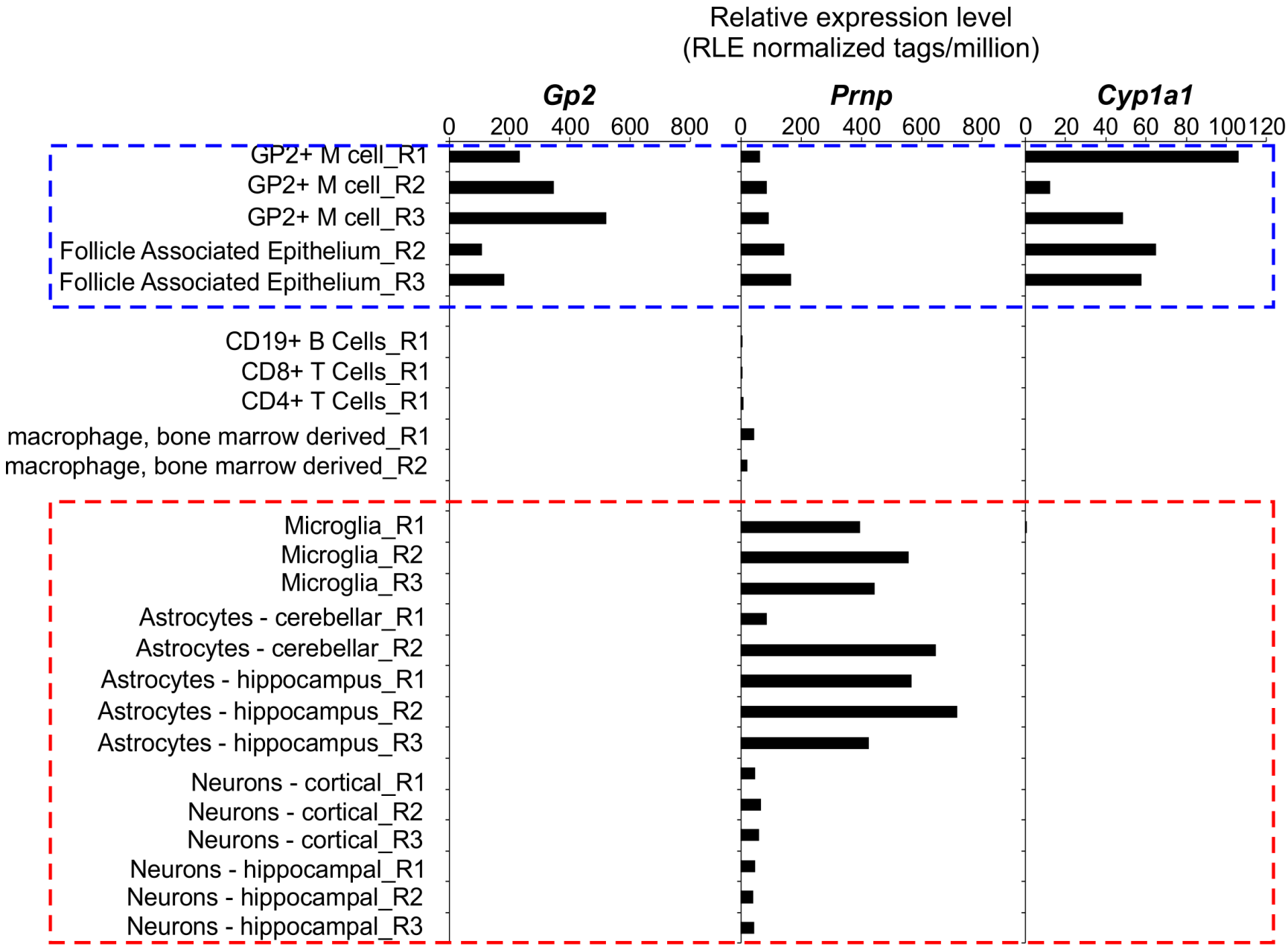

Marshall Fig.1